June 2009 Volume 5 Issue 3

Trade Science Inc.

Materials Science

An Indian Journal

Full Paper

MSAIJ, 5(3), 2009 [258-266]

Erosion wear behavior of TiO_2 filled glass fiber reinforced epoxy composites

Sandhyarani Biswas[1]*, Subhrajit Ray[1], Alok Satapathy[1], Amar Patnaik[2]

[1]Mechanical Engineering Department, N.I.T.Rourkela-769008, (INDIA)

[2]Mechanical Engineering Department, N.I.T.Hamirpur-177005, (INDIA)

E-mail : biswas.sandhya@gmail.com

Received: 19th May, 2009 ; Accepted: 24th May, 2009

ABSTRACT

This paper describes the development and characterization of a new set of glass fiber reinforced epoxy composites filled with TiO_2 particulate/filler. The newly developed composites are characterized with respect to their mechanical and erosion wear characteristics. Experiments are carried out to study the effect of fiber content, impact velocity, impingement angle, stand-off distance and erodent size on the solid particle erosion behaviour of these composites. The significant control factors and their interactions predominantly influencing the wear rate are identified by using Taguchi experimental design. The study reveals that the fiber content, impact velocity, impingement angle and erodent size have substantial influence in determining the rate of material loss from the composite surface due to erosion. Then, Arti?cial neural network (ANN) technique has been use to predict the erosion rate based on the experimentally measured database of composites. Also the morphology of eroded surfaces is examined by using scanning electron microscopy (SEM) and possible erosion mechanisms are discussed.

KEYWORDS

Glass fiber;
Epoxy resin;
Erosion wear;
TiO_2;
Taguchi method;
ANN.

1. INTRODUCTION

Polymer and their composites are finding ever increasing usage for numerous industrial applications such as bearing material, rollers, seals, gears, cams, wheels, clutches and transmission belts etc. Erosive wear in such applications caused by abrasive particles is a major industrial problem. Therefore a full understanding of the effects of all system variables on the wear rate is necessary in order to undertake appropriate steps in the design of machine or structural component and in the choice of materials to reduce/control wear. Solid particle erosion is the progressive loss of original material from a solid surface due to mechanical interaction between that surface and solid particles. There have been various reports of applications of polymers and their composites in erosive wear situations in the literature[1-2]. Solid particle erosion of polymers and their composites have not been investigated to the same extent as for metals or ceramics. However, a number of researchers have evaluated the resistance of various types of polymers and their composites to solid particle erosion. Materials that have been eroded include nylon[3,4], polystyrene[5], epoxy[6,7], polypropylene[8], ultrahigh molecular weight polyethylene[9], polyetheretherketone (PEEK)[10], rubber[11-13], elastomers[14-19] and various polymer based composites[20-24]. Their erosion rates are considerably higher than metals. However, elastomers and rubbers are being used as protective coatings for erosion resistance[13]. The erosion resistance of polymers is two or three orders of magnitude lower than that of metallic materials. Also, it is well known that the

erosion rate of polymer composites is usually higher than that of neat polymers. The most important factor for design with composites is the fibre content/loading, as it controls the mechanical and thermo-mechanical properties. In order to obtain the desired material properties for a particular application, it is important to know how the material performance changes with the fibre content under given loading conditions. The solid particle erosion behaviour of polymer composites as a function of fibre content has been studied to a limited extent[21,23]. A literature survey showed that a few studies have been carried out on the solid particle erosion behaviour of glass fiber reinforced epoxy based composites filled with ceramic fillers particularly TiO_2. Advantage of adding filler into composites is to reduce the cost and also improves the performance of composite. Hence, a comprehensive and systematic study of erosion behaviour of glass fiber reinforced epoxy based composites filled with TiO_2 is required.

In view of the above, the objective of the present investigation was to study the solid particle erosion behaviour of glass fiber reinforced epoxy based composites filled with TiO_2 filler and hence mechanical properties. The significant control factors and their interactions predominantly influencing the wear rate are identified by using Taguchi experimental design. Also Arti?cial neural network (ANN) technique has been use to predict the erosion rate based on the experimentally measured database of composites.

2. EXPERIMENTAL

2.1. Specimen preparation

Cross plied E-glass fibers (360 roving taken from Saint Gobian) are reinforced with Epoxy LY 556 resin, chemically belonging to the 'epoxide' family is used as the matrix material. Its common name is Bisphenol A Diglycidyl Ether. The low temperature curing epoxy resin (Araldite LY 556) and corresponding hardener (HY951) are mixed in a ratio of 10:1 by weight as recommended. The epoxy resin and the hardener are supplied by Ciba Geigy India Ltd. E-glass fiber and epoxy resin has modulus of 72.5 GPa and 3.42GPa respectively and possess density of 2590 kg/m^3 and 1100kg/m^3 respectively. The filler material TiO_2 (density 4.2 gm/cm^3) is provided by NICE Ltd India sieved to obtain particle size in the range 70-90 μm. Composites of three different compositions such as 30wt%, 40wt% and 50wt% glass fiber are made and the filler content (weight fraction of TiO_2 in the composite) is kept at 10% for all the samples and the designations of these composites are given in TABLE 1. The castings are put under load for about 24 hours for proper curing at room temperature. Specimens of suitable dimension are cut using a diamond cutter for physical characterization and erosion test.

TABLE 1: Designation of composites

Composites	Compositions
C_1	Epoxy (60wt%)+Glass Fiber (30wt%)+TiO_2 (10wt%)
C_2	Epoxy (50wt%)+Glass Fiber (40wt%)+TiO_2 (10wt%)
C_3	Epoxy (40wt%)+Glass Fiber (50wt%)+TiO_2 (10wt%)

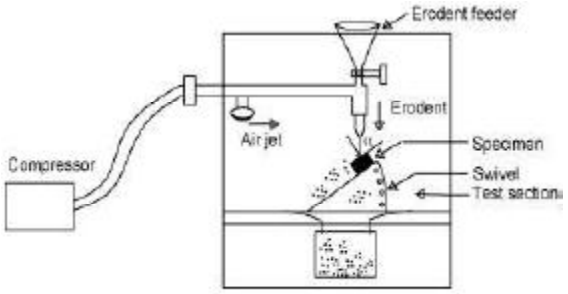

Figure 1 : Schematic diagram of the erosion test rig

2.2. Test apparatus

Figure 1 shows the schematic diagram of erosion test rig confirming to ASTM G 76. The set up is capable of creating reproducible erosive situations for assessing erosion wear resistance of the prepared composite samples. It consists of an air compressor, an air particle mixing chamber and an accelerating chamber. Dry compressed air is mixed with the particles which are fed at constant rate from a sand flow control knob through the nozzle tube and then accelerated by passing the mixture through a convergent brass nozzle of 3 mm internal diameter. These particles impact the specimen which can be held at various angles with respect to the direction of erodent flow using a swivel and an adjustable sample clip. The velocity of the eroding particles is measured using double disc method. In the present study, dry silica sand (angular) of different particle sizes (400, 500 and 600 μm) is used as erodent. Each sample is cleaned in acetone, dried and weighed to an accuracy of ±0.1 mg using a precision electronic balance. It is then eroded in the test rig for 30 min and

weighed again to determine the weight loss. The process is repeated till the erosion rate attains a constant value called steady-state erosion rate. The ratio of this weight loss to the weight of the eroding particles causing the loss is then computed as a dimensionless incremental erosion rate. The erosion rate is defined as the weight loss of the specimen due to erosion divided by the weight of the erodent causing the loss.

2.3. Taguchi experimental analysis

Design of experiment is a powerful analysis tool for modeling and analyzing the influence of control factors on performance output. The most important stage in the design of experiment lies in the selection of the control factors. Therefore, a number of factors are included so that non-significant variables can be identified at earliest opportunity. The wear tests are carried out under operating conditions given in TABLE 2.

The tests are conducted at room temperature as per experimental design given in TABLE 3. Five parameters viz., velocity of impact, fiber loading, stand off distance, impingement angle and erodent size each at three levels, are considered in this study in accordance with L_{27} (3^{13}) orthogonal array design. In TABLE 3, each column represents a test parameter and a row gives a test condition which is nothing but a combination of parameter levels. The experimental observations are transformed into signal-to-noise (S/N) ratios. There are several S/N ratios available depending on the type of characteristics. The S/N ratio for minimum wear rate coming under smaller is better characteristic, which can be calculated as logarithmic transformation of the loss function as shown below.

Smaller is the better characteristic $\frac{S}{N} = -10\log\frac{1}{n}\left(\sum y^2\right)$

where n is the number of observations, and y is the observed data. "Lower is better" (LB) characteristic, with the above S/N ratio transformation, is suitable for minimization of wear rate.

TABLE 2: Levels of the variables used in the experiment

Control factor	Level			
	I	II	III	Units
A: Velocity of impact	45	65	85	m/sec
B: Fiber loading	30	40	50	%
C: Stand off distance	120	180	240	mm
D: Impingement angle	30	60	90	degree
E: Erodent size	400	500	600	μm

TABLE 3: Orthogonal array for L_{27} (3^{13}) Taguchi's experimental design

$L_{27}(3^{13})$	1	2	3	4	5	6	7	8	9	10	11	12	13
	A	B	$(AxB)_1$	$(AxB)_2$	C	$(BxC)_1$	$(BxC)_2$	$(AxC)_1$	D	E	$(AxC)_2$		
1	1	1	1	1	1	1	1	1	1	1	1	1	1
2	1	1	1	1	2	2	2	2	2	2	2	2	2
3	1	1	1	1	3	3	3	3	3	3	3	3	3
4	1	2	2	2	1	1	1	2	2	2	3	3	3
5	1	2	2	2	2	2	2	3	3	3	1	1	1
6	1	2	2	2	3	3	3	1	1	1	2	2	2
7	1	3	3	3	1	1	1	3	3	3	2	2	2
8	1	3	3	3	2	2	2	1	1	1	3	3	3
9	1	3	3	3	3	3	3	2	2	2	1	1	1
10	2	1	2	3	1	2	3	1	2	3	1	2	3
11	2	1	2	3	2	3	1	2	3	1	2	3	1
12	2	1	2	3	3	1	2	3	1	2	3	1	2
13	2	2	3	1	1	2	3	2	3	1	3	1	2
14	2	2	3	1	2	3	1	3	1	2	1	2	3
15	2	2	3	1	3	1	2	1	2	3	2	3	1
16	2	3	1	2	1	2	3	3	1	2	2	3	1
17	2	3	1	2	2	3	1	1	2	3	3	1	2
18	2	3	1	2	3	1	2	2	3	1	1	2	3
19	3	1	3	2	1	3	2	1	3	2	1	3	2
20	3	1	3	2	2	1	3	2	1	3	2	1	3
21	3	1	3	2	3	2	1	3	2	1	3	2	1
22	3	2	1	3	1	3	2	2	1	3	3	2	1
23	3	2	1	3	2	1	3	3	2	1	1	3	2
24	3	2	1	3	3	2	1	1	3	2	2	1	3
25	3	3	2	1	1	3	2	3	2	1	2	1	3
26	3	3	2	1	2	1	3	1	3	2	3	2	1
27	3	3	2	1	3	2	1	2	1	3	1	3	2

The standard linear graph, as shown in figure 2, is used to assign the factors and interactions to various columns of the orthogonal array[25].

The plan of the experiments is as follows: the first column is assigned to impact velocity (A), the second column to fiber loading (B), the fifth column to stand-off distance (C), ninth column to impingement angle (D) and twelfth column to erodent size (E). The remaining columns are assigned similarly according to the design.

2.4. Neural computation

Erosion wear process is considered as a non-linear problem with respect to its variables: either materials or operating conditions. To obtain minimum wear rate, combinations of operating parameters have to be planned. Therefore a robust methodology is needed to study these interrelated effects. In this work, a statistical method, responding to the constraints, is implemented to correlate the operating parameters. This methodology is based on artificial neural networks (ANN), which is a technique that involves database training to predict input-output evolutions. The details of this methodology are described by Rajasekaran and Pai[26]. In the present analysis, the velocity of impact, fiber content, stand-off distance, impingement angle and erodent size are taken as the five input parameters. Each of these parameters is characterized by one neuron and consequently the input layer in the ANN structure has five neurons. The database is built considering experiments at the limit ranges of each parameter. Experimental result sets are used to train the ANN in order to understand the input-output correlations. The database is then divided into three categories, namely: (i) a validation category, which is required to define the ANN architecture and adjust the number of neurons for each layer. (ii) a training category, which is exclusively used to adjust the network weights and (iii) a test category, which corresponds to the set that validates the results of the training protocol. The input variables are normalized so as to lie in the same range group of 0-1. The outer layer of the network has only one neuron to represent wear rate. To train the neural network used for this work, about 135 data sets obtained during erosion trials on different composites are taken. Different ANN structures (Input-Hidden-Output nodes) with varying number of neurons in the hidden layer are tested at constant cycles, learning rate, error tolerance, momentum parameter, noise factor and slope parameter. Based on least error criterion, one structure, shown in TABLE 4, is selected for training of the input-output data. A software package NEURALNET for neural computing developed by Rao and Rao[27] using back propagation algorithm is used as the prediction tool for erosion wear rate of different composites under various test conditions. The three-layer neural network having an input layer (I) with five input nodes, a hidden layer (H) with twelve neurons and an output layer (O) with one output node employed for this work is shown in figure 3.

TABLE 4: A typical case of input parameters selected for training

Input parameters for training	Values
Error tolerance	0.01
Learning rate (ß)	0.01
Momentum parameter(α)	0.03
Noise factor (NF)	0.01
Number of epochs	20,0000
Slope parameter (£)	0.6
Number of hidden layer	12
Number of input layer neuron (I)	5
Number of output layer neuron (O)	1

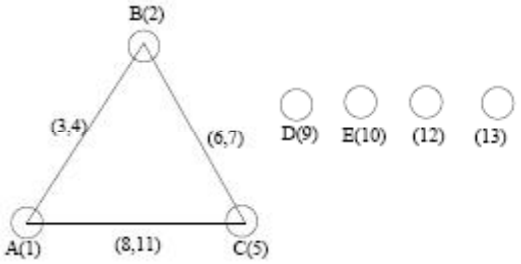

Figure 2 : Linear graphs for L_{27} array

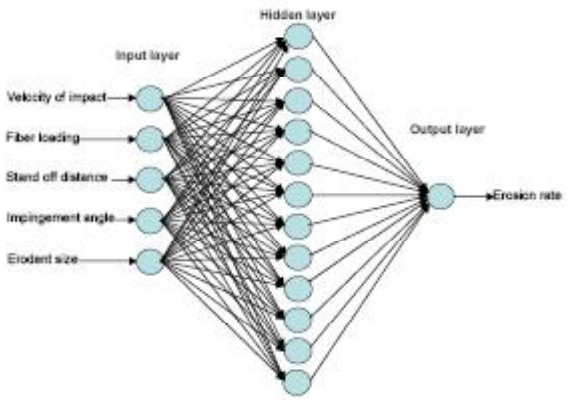

Figure 3 : Neural network architecture

3. RESULTS AND DISCUSSION

3.1. Mechanical characterization of composites

The most important factor for design with compos-

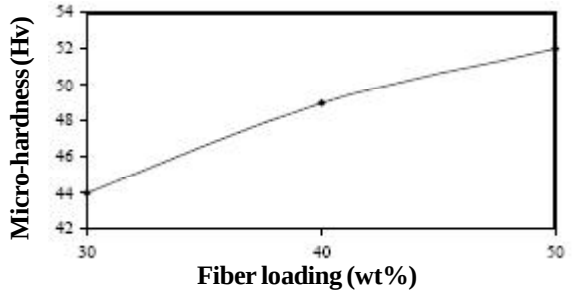

Figure 4: Variation of micro-hardness of the composites with the fiber loading

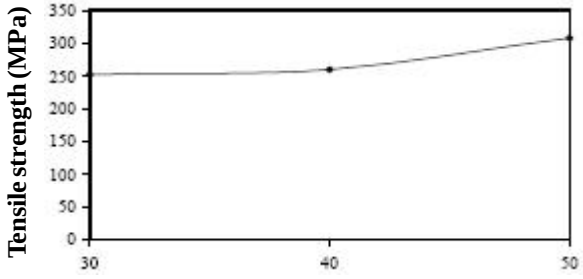

Figure 5: Effect of fiber loading on tensile strength of composites

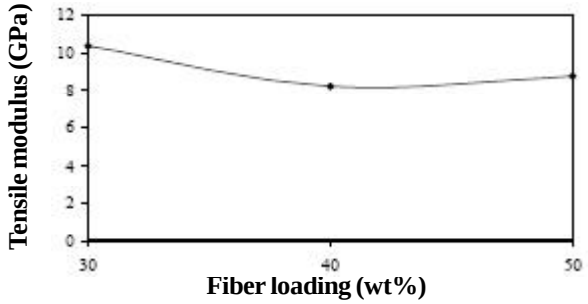

Figure 6: Effect of fiber loading on tensile modulus of composites

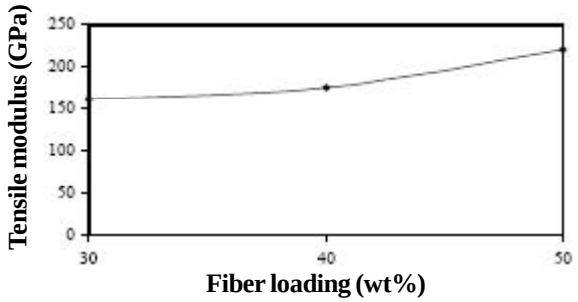

Figure 7: Effect of fiber loading on flexural strength of composites

ites is the fibre content, as it controls the mechanical and thermo-mechanical properties.

3.1.1. Effect of fiber loading on micro-hardness

The measured hardness values of all the three composites are presented in figure 4. It can be seen that the hardness is increasing with the increase in fiber loading at constant filler content. In case of composites with fiber loading up to 50 wt% gives higher value of micro-hardness as compared to 30wt% composite. When the increase in fiber loading the formation of air bubbles and void in composites decreases causing homogeneity in microstructure and affect the mechanical properties.

3.1.2. Effect of fiber loading on tensile properties

The test results for tensile strengths and moduli are shown in figures 5 and 6, respectively. It is seen that in all the samples irrespective of the constant filler material the tensile strength of the composite increases with increase in fiber loading. There can be two reasons for this increase in the strength properties of these composites compared. One possibility is that the chemical reaction at the interface between the filler particles and the matrix may be too strong to transfer the tensile stress; the other is that at constant filler content with the increase in fiber loading result in stress concentration in the glass fiber reinforced epoxy composite. These two factors are responsible for increase in the tensile strengths of the composites so significantly. From figure 4 it is clear that with the increase in fiber loading the tensile moduli of the glass epoxy composites decrease gradually.

3.1.3. Effect of fiber loading on flexural strength

Figure 7 shows the comparison of flexural strengths of the composites obtained experimentally from the bend tests. It is interesting to note that flexural strength increases with increase in fiber loading from 30-50wt% of glass epoxy composite structure.

3.1.4. Effect of fiber loading on impact strength

The impact energy values of different composites recorded during the impact tests are given in TABLE 5. It shows that the resistance to impact loading of glass epoxy composites improves with increase in fiber loading as shown in figure 8. High strain rates or impact loads may be expected in many engineering applications of composite materials. The suitability of a composite for such applications should therefore be determined not only by usual design parameters, but by its

impact or energy absorbing properties.

3.2. Erosion characteristics of composites

3.2.1. Experimental analysis

The analysis is made using the popular software specifically used for design of experiment applications known as MINITAB 14. From TABLE 5, the overall mean for the S/N ratio of the erosion rate is found to be -49.02 db.

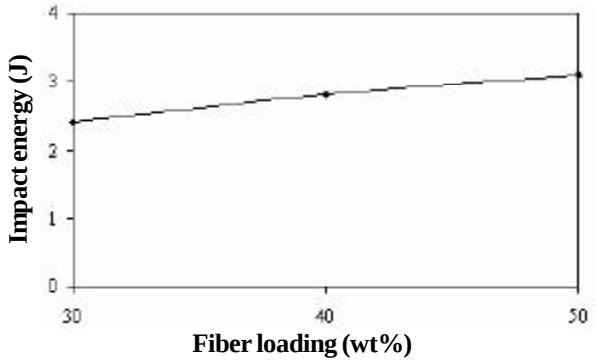

Figure 8: Effect of fiber loading on impact strength of composites

Figure 9 shows graphically the effect of the five control factors on erosion rate. Before any attempt is made to use this simple model as a predictor for the measures of performance, the possible interactions between the control factors must be considered. Thus factorial design incorporates a simple means of testing for the presence of the interaction effects. Analysis of the result leads to the conclusion that factor combination of A_1, B_2, C_3, D_2 and E_2 gives minimum erosion rate. As for as minimization of erosion rate is concerned, factors A, B, D and E have significant effect whereas factor C has least effect as shown in figure 9. It is also observed from figure that the significant level of each factor for minimization of erosion rate. The interaction graphs are shown in the Figures 10, 11 and 12.

The experimental erosion wear rate (E_{expt}) of the TiO_2 filled glass fiber reinforced epoxy composites are calculated as given in TABLE 5. Seventy five percent of data collected from erosion test is used for training whereas twenty five percent data is used for testing. The parameters of three layer architecture of ANN model are set as input nodes = 5, output node = 1,

TABLE 5: Experimental design using L_{27} orthogonal array

Expt. no.	Impact velocity (A)m/sec	Fiber content(B) %	Stand-off distance(C) mm	Impingement angle(D) degree	Erodent size (E) μm	Erosionrate (Er)mg/kg	S/N ratio(db)
1	45	30	120	30	400	290.43	-49.26
2	45	30	180	60	500	245.45	-47.8
3	45	30	240	90	600	226.34	-47.1
4	45	40	120	60	500	195.71	-45.83
5	45	40	180	90	600	282.84	-49.03
6	45	40	240	30	400	264.94	-48.46
7	45	50	120	90	600	394.12	-51.91
8	45	50	180	30	400	281.42	-48.99
9	45	50	240	60	500	178.58	-45.04
10	65	30	120	60	600	325.61	-50.25
11	65	30	180	90	400	356.88	-51.05
12	65	30	240	30	500	245.43	-47.8
13	65	40	120	90	400	249.45	-47.94
14	65	40	180	30	500	258.83	-48.26
15	65	40	240	60	600	242.16	-47.68
16	65	50	120	30	500	234.75	-47.41
17	65	50	180	60	600	339.37	-50.61
18	65	50	240	90	400	378.19	-51.55
19	85	30	120	90	500	407.20	-52.2
20	85	30	180	30	600	228.26	-47.17
21	85	30	240	60	400	246.19	-47.83
22	85	40	120	30	600	268.49	-48.58
23	85	40	180	60	400	332.80	-50.44
24	85	40	240	90	500	208.56	-46.38
25	85	50	120	60	400	352.17	-50.94
26	85	50	180	90	500	420.58	-52.48
27	85	50	240	30	600	369.54	-51.35

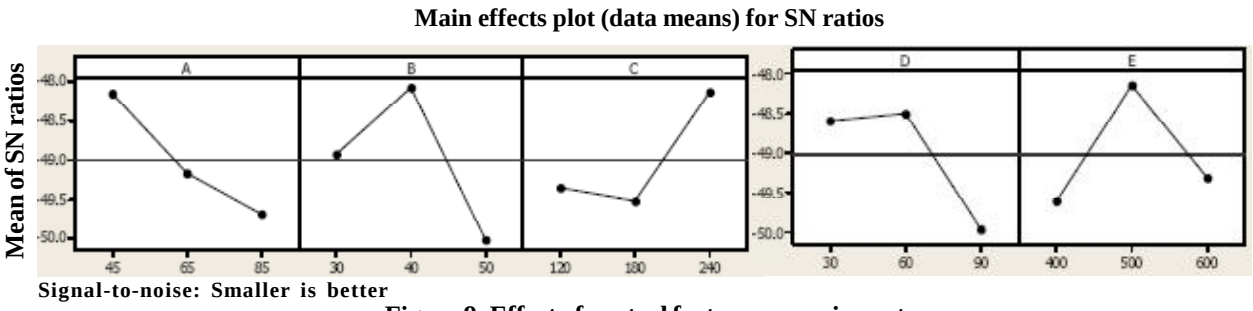

Figure 9: Effect of control factors on erosion rate

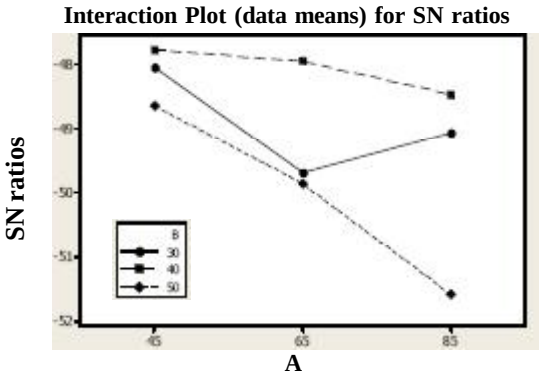

Figure 10: Interaction graph between A×B for erosion rate

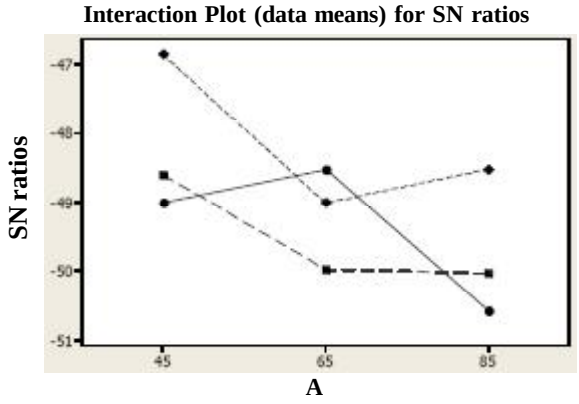

Figure 11: Interaction graph between A×C for erosion rate

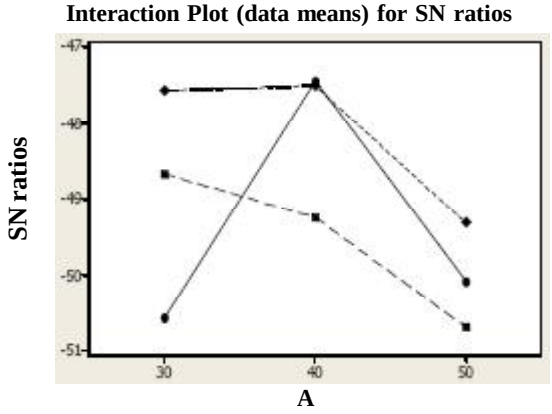

Figure 12: Interaction graph between B×C for erosion rate

hidden nodes = 12, learning rate = 0.01, momentum parameter = 0.03, number of epochs = 20, 0000 and a set of predicted output (E_{rANN}) is obtained. TABLE 6 a comparison between the experimental and the ANN predicted results. The errors calculated with respect to the theoretical results are also given. It is observed that maximum error between ANN prediction and experimental wear rate is 0-12%. The error in case of ANN model can further be reduced if number of test patterns is increased. However, present study demonstrates application of ANN for prediction of wear rate in a complex process of solid particle erosion of polymer composites.

3.2.2. Steady state erosion

Erosion behaviour of the composites is generally ascertained by correlating erosion rate with impingement angle, erodent velocity and erodent particle size. Erosion behaviour strongly depends on impingement angle. Ductile behaviour is characterized by maximum erosion rate and generally occurs at 15-30. Brittle behaviour is characterized by maximum erosion rate at 90^0C. Semi-ductile behaviour is characterized by the maximum erosion rate at 45-60^0C. Thus the erosion wear behaviour of polymer composites can be grouped into ductile and brittle categories although this grouping is not definitive because the erosion characteristics equally depend on the experimental conditions as on composition of the target material. The results are presented in figure 13 which shows the peak erosion taking place at an impingement angle of 60^0C for the filled composites. This clearly indicates that these composites respond to solid particle impact neither in a purely shows semi-ductile behaviour as per literature. This behaviour can be termed as semi-ductile in nature which may be attributed to the incorporation of glass fibers

TABLE 6: Comparison of experimental result and ANN results

Expt. no.	$E_{rexpt.}$(mg/kg)	E_{rANN}(mg/kg)	Error (%)
1	290.43	245.33	6.85191
2	245.45	203.95	9.57425
3	226.34	176.93	6.88787
4	195.71	111.31	9.91262
5	282.84	230.34	4.41946
6	264.94	204.54	1.73624
7	394.12	286.33	10.8571
8	281.42	193.51	8.14085
9	178.58	127.07	7.55404
10	325.61	224.53	11.0807
11	356.88	302.1	2.86371
12	245.43	173.76	2.71767
13	249.45	168.65	6.33393
14	258.83	186.49	2.83583
15	242.16	156.04	8.72150
16	234.75	178.27	3.62939
17	339.37	262.33	3.54775
18	378.19	286.06	7.17364
19	407.20	307.29	8.57318
20	228.26	183.82	9.00727
21	246.19	171.43	3.96441
22	268.49	233.62	11.2224
23	332.80	232.37	10.6461
24	208.56	164.48	10.0307
25	352.17	264.4	6.46562
26	420.58	326.23	6.97845
27	369.54	298.25	1.70211

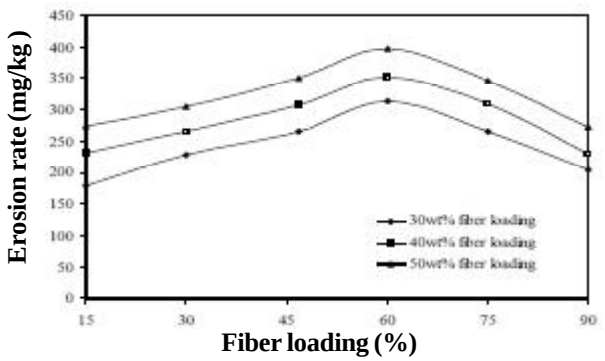

Figure 13: Variation of erosion rate with impingement angle

and TiO_2 particles within the epoxy body.

3.2.3. Surface morphology

Generally surface morphology of eroded surfaces indicates whether erosion has occurred by a ductile or brittle mechanism. Hence scanning electron microscopy (SEM) studies have been done to ascertain the wear mechanism at 30^0C, 60^0C and 90^0C impact angles. Figure 14 show micrographs of eroded surfaces of 30wt% of the composite at 30^0C impact angles at impact velocity of 65 m/s. It is evident from the micrographs (Figure 14a, b) that the material removal in composite with 30wt% fiber loading is dominated by micro-ploughing, micro-cutting and plastic deformation. The plastically deformed material subsequently removed from the surface by micro-cutting leads to maximum wear at 30^0C impact angle; most material is lost when a maximum strain in the target is exceeded. Under normal impact, formation of micro-cracks and embedment of fragments of sand particles in composite with 40wt% fiber loading is evident from the micrographs (Figure 15). Micrograph (Figure 15a, b) con?rms the brittle nature of the composite with deeper micro-cracks. However, the normal impact did not result in higher erosion rate like brittle materials. During normal impact the largest part of the initial energy is converted in to heat and hence matrix is softened which resulted in embedment of sand particles. The embedded sand particles control the further erosion of the target surface.

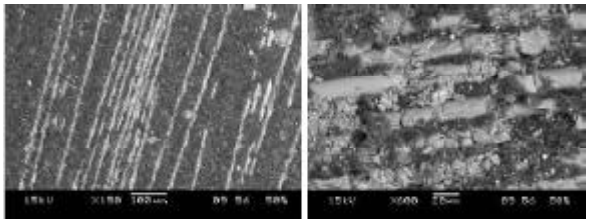

(A) **(B)**

Figure 14 : SEM of 30wt% fiber loading composite

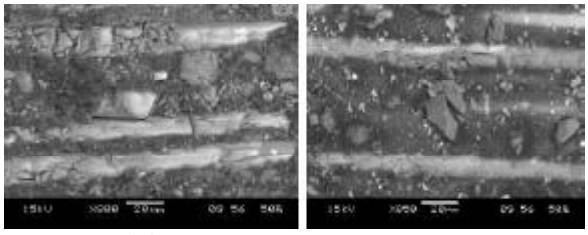

(A) **(B)**

Figure 15: SEM of 40wt% fiber loading composite

Figure 16a, b show micrographs of eroded surfaces of 50wt% glass fiber reinforced epoxy composite. At oblique impact angle, micrographs (Figure 16a) shows matrix is plastically deformed and amount of deformation is proportional to impact velocity of particles. At lower impact velocity removal of matrix along the length of the fiber and subsequently exposed fiber getting removed can be seen from the micrograph (Figure 16b).

Full Paper

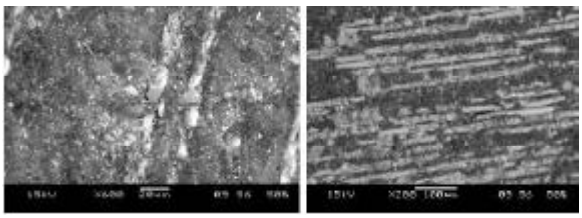

(A) (B)

Figure 16: SEM of 50wt% fiber loading composite

4. CONCLUSIONS

This analytical and experimental investigation into the erosion behaviour of TiO_2 filled glass-epoxy composites leads to the following conclusions:

- This work shows that successful fabrication of a glass fiber reinforced epoxy composites with constant filler content by simple hand lay-up technique and it is noticed that there is significant improvement in the mechanical properties of the composites with the increase in fiber loading.
- Solid particle erosion characteristics of these composites can be successfully analyzed using Taguchi experimental design scheme. Taguchi method provides a simple, systematic and efficient methodology for the optimization of the control factors.
- Study of influence of impingement angle on erosion rate of the composites with different percentage of fiber loading reveals their semi-ductile nature with respect to erosion wear. The peak erosion rate is found to be occurring at 60^0C impingement angle under the various experimental conditions.
- SEM studies reveal that material removal takes place by microcutting, plastic deformation, and microcracking, exposure of ?bers and removal of the fiber.
- Artificial neural network technique was applied to predict the erosion rate of composites. The results show that the predicted data a re well acceptable when comparing them to measured values. The predicted property profiles as a function of fiber content and testing conditions proved a remarkable capability of well-trained neural networks for modeling concern.

REFERENCES

[1] K.V.Pool, C.K.H.Dharan, I.Finnie; Wear, **107**, 1 **(1986)**.

[2] S.M.Kulkarani, Kishore; Polym.Polym.Comp., **9**, 25 **(2001)**.

[3] G.P.Tilly; Wear, **14**, 63 **(1969)**.

[4] G.P.Tilly, W.Sage; Wear, **16**, 447 **(1970)**.

[5] C.M.Thai, K.Tsuda, H.Hojo; J.Testing Eval., **9**, 359 **(1981)**.

[6] N.Miyazaki, T.Hamao; J.Comp.Mater., **30**, 35 **(1996)**.

[7] N.M.Barkoula, J.Karger-Kocsis; J.Reinforced Plast.Comp., **19**, 1 **(2000)**.

[8] S.M.Walley, J.E.Field, P.Yennadhiou; Wear, **100**, 263 **(1984)**.

[9] Y.Q.Wang, L.P.Huang, W.L.Liu, J.Li; Wear, **218**, 128 **(1998)**.

[10] S.M.Walley, J.E.Field, M.Greengrass; Wear, **114**, 59 **(1987)**.

[11] G.M.Bartenev, N.S.Penkin; Sov.J.Friction Wear, **1**, 10 **(1980)**.

[12] N.S.Penkin; Sov.J.Friction Wear, **2**, 56 **(1981)**.

[13] N.S.Penkin; Sov.J.Friction Wear, **3**, 55 **(1982)**.

[14] N.N.Goloshchapov, N.S.Penkin; Sov.J.Friction Wear, **10**, 8 **(1989)**.

[15] V.N.Kurachenkov, S.A.Kizhaev, M.P.Letunovskii, V.V.Strakhov, V.N.Anisimov, S.F.Egorov; Sov.J. Friction Wear, **11**, 132 **(1990)**.

[16] N.M.Barkoula, J.Gremmels, J.Karger-Kocsis; Wear, **247**, 100 **(2001)**.

[17] J.Li, I.M.Hutchings; Wear, **135**, 293 **(1990)**.

[18] J.C.Arnold, I.M.Hutchings; J.Nat.Rubb.Res., **6**, 241 **(1991)**.

[19] I.M.Hutchings, D.W.T.Deuchar, A.H.Muhr; J. Mater.Sci., **22**, 4071 **(1987)**.

[20] M.Roy, B.Vishwanathan, G.Sundararajan; Wear, **171**, 149 **(1994)**.

[21] N.Miyazaki, T.Hamao; J.Comp.Mater., **28**, 871 **(1994)**.

[22] K.R.Karasek, K.C.Goretta, D.A.Helberg, J.L. Routbort; J.Mater.Sci.Lett., **11**, 1143 **(1992)**.

[23] N.M.Barkoula, J.Karger-Kocsis; Wear, **252**, 80 **(2002)**.

[24] U.S.Tewari, A.P.Harsha, A.M.Häger, K.Friedrich; Wear, **252**, 992 **(2002)**.

[25] S.P Glen; 'Taguchi Methods: A Hands-on Approach', Addison-Wesley, **(1993)**.

[26] S.Rajasekaran, G.A.Vijayalakshmi Pai; 'Neural Networks, Fuzzy Logic And Genetic Algorithms-Synthesis and Applications', Prentice Hall of India Pvt.Ltd., New Delhi, **(2003)**.

[27] V.Rao, H.Rao; 'C++ Neural Networks and Fuzzy Systems', BPB Publications, **(2000)**.